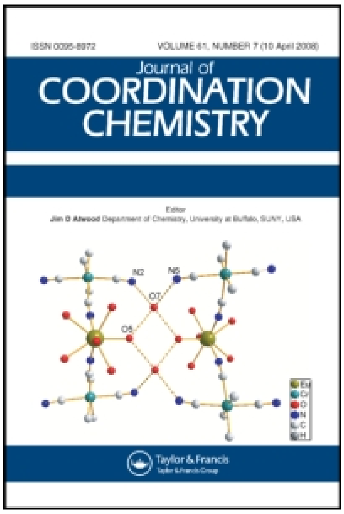

Journal of Coordination Chemistry
Publication details, including instructions for authors and subscription information:
http://www.informaworld.com/smpp/title~content=t713455674

Hydrothermal syntheses, crystal structures and thermal properties of open-structure materials, Pr(III)-succinate complexes with 3D networks

Xing Jing Zhang[ab]; Yong Heng Xing[a]; Jing Han[a]
[a] College of Chemistry and Chemical Engineering, Liaoning Normal University, Dalian, China [b] College of Chemistry, Jilin Normal University, Siping, China

To cite this Article Zhang, Xing Jing , Xing, Yong Heng and Han, Jing(2008) 'Hydrothermal syntheses, crystal structures and thermal properties of open-structure materials, Pr(III)-succinate complexes with 3D networks', Journal of Coordination Chemistry, 61: 5, 651 — 660, First published on: 18 June 2007 (iFirst)

To link to this Article: DOI: 10.1080/00958970701376309

URL: http://dx.doi.org/10.1080/00958970701376309

Journal of Coordination Chemistry
Vol. 61, No. 5, 10 March 2008, 651–660

Taylor & Francis
Taylor & Francis Group

Hydrothermal syntheses, crystal structures and thermal properties of open-structure materials, Pr(III)-succinate complexes with 3D networks

XING JING ZHANG†‡, YONG HENG XING*† and JING HAN†

†College of Chemistry and Chemical Engineering, Liaoning Normal University,
Huanghe Road #850, Dalian, China, 116029
‡College of Chemistry, Jilin Normal University, Shida Road #1301,
Siping, China, 136000

(*Received 28 April 2007; in final form 3 May 2007*)

Rare-earth dicarboxylate open structure materials $\{[Pr(H_2O)]_2[O_2C(CH_2)_2CO_2]_3\}_n$ (**1**) and $\{[Pr(H_2O)]_2[O_2C(CH_2)_2CO_2]_3 \cdot H_2O\}_n$ (**2**) have been synthesized by reaction of succinic acid with nitrate salts of Pr(III) under hydrothermal conditions (150°C, 4 days). Complex **1** crystallizes in the triclinic space group $P\bar{1}$ with $a = 7.8828(8)$ Å, $b = 8.1247(8)$ Å, $c = 14.2271(14)$ Å, $\alpha = 96.907(2)^\circ$, $\beta = 96.962(2)^\circ$, $\gamma = 103.600(2)^\circ$, and $Z = 2$. Complex **2** is in the monoclinic space group $C2/c$ with $a = 20.104(4)$ Å, $b = 7.9343(16)$ Å, $c = 14.013(3)$ Å, $\beta = 121.08(3)$, and $Z = 4$. X-ray diffraction analysis reveals that the complexes are constructed by succinic acid bridging the chains of edge-sharing $PrO_8(H_2O)$ polyhedra to form 3D network structures. **1** and **2** possess different topological structures due to the difference in the conformations of coordinated succinic acid. Thermal decomposition kinetics of **1** and **2** are also discussed in detail. Non-thermal kinetic decomposition shows that, for **1**, the possible reaction mechanisms of the three steps are three dimensional pervasion with $n = 2$, nucleation and growth with $n = 1/4$, nucleation and growth with $n = 1/4$, respectively, and the kinetic equations may be expressed as $\mathrm{d}\alpha/\mathrm{d}T = (A/\beta)\exp(-E/\mathrm{RT})\{3/2(1-\alpha)^{2/3}[1-(1-\alpha)^{1/3}]^{-1}\}$, $\mathrm{d}\alpha/\mathrm{d}T = (A/\beta)\exp(-E/\mathrm{RT})\{1/4(1-\alpha)[-\ln(1-\alpha)]^{-3}\}$, and $\mathrm{d}\alpha/\mathrm{d}T = (A/\beta)\exp(-E/\mathrm{RT})\{1/4(1-\alpha)[-\ln(1-\alpha)]^{-3}\}$, respectively; for **2**, the possible reaction mechanisms of the three steps are nucleation and growth with $n = 1/4$, chemical reaction, nucleation and growth with $n = 1$. Kinetic equations may be expressed as $\mathrm{d}\alpha/\mathrm{d}T = (A/\beta)\exp(-E/\mathrm{RT})\{1/4(1-\alpha)[-\ln(1-\alpha)]^{-3}\}$, $\mathrm{d}\alpha/\mathrm{d}T = (A/\beta)\exp(-E/\mathrm{RT})[(1-\alpha)^2]$, and $\mathrm{d}\alpha/\mathrm{d}T = (A/\beta)\exp(-E/\mathrm{RT})(1-\alpha)$.

Keywords: Praseodymium complexes; Succinic acid; Hydrothermal synthesis; Crystal structure; Thermal properties

1. Introduction

Preparation of new open-structure materials is justified by potential applications as functional materials and also by intriguing topological structures [1–8]. Most work

---

*Corresponding author. Email: yhxing2000@yahoo.com

Journal of Coordination Chemistry
ISSN 0095-8972 print/ISSN 1029-0389 online © 2008 Taylor & Francis
DOI: 10.1080/00958970701376309

has focused on the transition metals. However, use of lanthanide metals in assembling open-structure materials has surged [9] due to their special magnetic, catalytic and luminescent properties. Non-transition metal phosphate complexes have been reported with various structural types. For example, Férey *et al.* prepared some gallium and aluminum-templated phosphates [10–12] to supplant zeolite-type materials as complexes with great pore sizes.

Using the hydrothermal method, open frameworks containing lanthanides may provide new materials with desirable properties. Multidentate N- or O-donor ligands have been extensively used in construction of such extended structures, especially multifunctional carboxylic acids [13–18]. Succinic acid is interesting due to conformational flexibility and coordination diversity. Although a few Ln-succinate complexes have been reported [19–24], exploitation of new synthetic methods, structures and functions in this system is still interesting. Detailed research of thermal decomposition kinetics for such complexes has not been reported. In this paper, syntheses, structures and thermal properties of $\{[Pr(H_2O)]_2[O_2C(CH_2)_2CO_2]_3\}_n$ and $\{[Pr(H_2O)]_2[O_2C(CH_2)_2CO_2]_3 \cdot H_2O\}_n$ are reported.

2. Experimental

2.1. *General*

All reagents were analytical grade and used as received without further purification. The infrared spectra were recorded on a JASCO FT/IR-480 PLUS Fourier Transform spectrometer with pressed KBr pellets in the range 200–4000 cm^{-1}.

The thermal analysis curves were recorded on a Perkin–Elmer Diamond TG/DTA. Carbon, hydrogen, and nitrogen analyses were performed on a Perkin–Elmer 240C automatic analyzer. Praseodymium was determined on a Plasma-Spec(I)-AES ICP automatic analyzer.

2.2. *Synthesis of 1 and 2*

2.2.1. $\{[Pr(H_2O)]_2[O_2C(CH_2)_2CO_2]_3\}_n$ (1). A mixture of 1 mmol $Pr(NO_3)_3 \cdot 6H_2O$, 1 mmol succinic acid, 3 mmol NaCl, and 2 mL 0.1 M NaOH aqueous solution in 15 mL water was sealed in a 25 mL Teflon-lined stainless reactor and heated at 150°C for 4 days under autogenous pressure, then cooled at 10°C/3 h to 100°C, followed by slow cooling to room temperature. Upon cooling to RT, the desired product appeared as light green granules in ca 10% (based on Pr) yield. Anal. Calcd for $C_{12}H_{16}O_{14}Pr_2$ (666.04): Pr: 42.31; C, 21.62; H: 2.40%. Found: Pr: 42.35; C: 21.65; H: 2.38%. IR data (KBr pellet, $\nu[cm^{-1}]$): 3435, 2981, 2925, 1563, 1448, 1402, 1303, 1214, 1175, 1049, 999, 974, 947, 905, 877, 809, 685, 647, 570, 524, 339, 285, 251, 235.

2.2.2. $\{[Pr(H_2O)]_2[O_2C(CH_2)_2CO_2]_3 \cdot H_2O\}_n$ (2). $\{[Pr(H_2O)]_2[O_2C(CH_2)_2CO_2]_3 \cdot H_2O\}_n$ has been reported [21], but the synthesis is different. By hydrothermal method, **2** was synthesized from the mixture of 1 mmol $Pr(NO_3)_3 \cdot 6H_2O$, 2 mmol succinic acid, 1 mmol phen, 0.004 mmol KOH and 15 mL H_2O in a 25 mL Teflon-lined stainless reactor heated under autogenous pressure (150°C, 4 days). The obtained light-green crystalline product was filtered off and dried at room temperature. Yield: 48% (based on Pr). Anal. Calcd for $C_{12}H_{18}O_{15}Pr_2$ (684.07): Pr: 41.20; C, 21.05; H: 2.63%. Found: Pr: 41.18; C: 21.11; H: 2.54%. IR data (KBr pellet, ν[cm^{-1}]): 3604, 3389, 2981, 2925, 1563, 1448, 1403, 1303, 1214, 1175, 1050, 999, 974, 947, 905, 877, 810, 685, 647, 570, 525, 339, 230.

2.3. *X-ray crystallography*

Suitable single crystals of both complexes were mounted on glass fibers for X-ray measurement. Reflection data were collected at room temperature on a Bruker AXS SMART APEX II CCD diffractometer with graphite-monochromated Mo-Kα radiation ($\lambda = 0.71073$ Å). Crystal structures were solved by the direct method and refined using SHELX-97. All non-hydrogen atoms were refined anisotropically; hydrogen atoms were placed at calculated positions and forced to ride on their carbon atoms with group Uiso values assigned. Atomic scattering factors and anomalous dispersion terms were taken from SHELX-97. Crystal data and details of the data collection and the structure refinement are given in table 1.

2.4. *Thermal analysis*

Thermal analysis was performed on a certain amount of powdered sample of each complex using a Perkin–Elmer Diamond TG/DTA. Thermal gravimetric

Table 1. Data collection conditions and refinement results for $\{[Pr(H_2O)]_2[O_2C(CH_2)_2CO_2]_3\}_n$.

Formula	$C_{12}H_{16}O_{14}Pr_2$
M(g mol^{-1})	666.04
Crystal system	Triclinic
Space group	$P\bar{1}$
a (Å)	7.8828(8)
b (Å)	8.1247(8)
c (Å)	14.2271(14)
α (°)	96.904(2)
β (°)	96.962(2)
γ (°)	103.600(2)
V (Å^3)	868.60(15)
Z	2
D_{Calcd}	2.531
Crystal size (mm^3)	0.15 × 0.05 × 0.20
$F(000)$	628
μ(Mo-Kα) (cm^{-1})	5.618
θ (°)	2.69–28.23
Reflections collected	5423
Independent reflections ($I > 2\sigma(I)$)	3749
Parameters	223
$\Delta(\rho)$ (e Å^{-3})	2.362 and −6.401
Goodness-of-fit	1.080
R^a	0.0595(0.0605)^b
$wR_2{}^a$	0.1490(0.1508)^b

[a] $R = \Sigma\|F_o| - |F_c\|/\Sigma|F_o$, $wR_2 = [\Sigma(w(F_o^2 - F_c^2)^2/[\Sigma(w(F_o^2)^2]^{1/2}$; $[F_o > 4\sigma(F_o)]$.
[b] Based on all data.

analyses (TGA) were carried out to examine the thermal stability of **1** and **2**. The samples were heated in N_2 at 1 atm with the heating rate of $10^{\circ}C\,min^{-1}$.

3. Results and discussion

3.1. *Syntheses*

Both complexes were synthesized by the hydrothermal method in H_2O system at lower reaction temperature than those in the recent report of Ln-succinate systems [23, 24]. While non-coordinated phen plays a direct role in the reaction system of **2**, only **1** is found in the absence of phen. In addition, $Pr(NO_3)_3 \cdot 6H_2O$ is used in our system, while $PrCl_3 \cdot 6H_2O$ was used previously [21, 23].

We attempted to synthesize new lanthanide complexes containing succinic acid ligand with neutral organic ligands such as phen, 2,2-bipy, 4,4-bipy etc. Our aim is that these neutral organic ligands could control the dimension of the molecular structure to get low dimension solid materials.

3.2. *IR spectroscopy*

The IR spectra of both complexes are similar, showing three characteristic spectral regions: (i) the strong absorption bands from 1402 to 1563 cm^{-1} for **1** and from 1403 to 1563 cm^{-1} for **2** can be assigned to the symmetric and asymmetric bands of C=O; (ii) a narrow band at 3606 and 3604 cm^{-1} in **1** and **2** is ν(O–H) of coordinated water; (iii) the range from 2925 to 2981 cm^{-1} is characteristic of the ν(C–H) vibrational modes of $–CH_2–$ groups within the carbon chain.

3.3. *Description of the crystal structures*

According to literature [19, 21, 23], **2** is isostructural with $\{[La(H_2O)]_2[O_2C(CH_2)_2CO_2]_3 \cdot H_2O\}_n$ [19] and $\{[Sm(H_2O)]_2[O_2C(CH_2)_2CO_2]_3 \cdot H_2O\}_n$ [23], and the same as that reported [21]. Complex **1** has important structural differences with **2**. For **1**, all carboxyl groups of succinic acids are deprotonated, in good agreement with the IR spectral data since no strong bands around 1702 cm^{-1} for –COOH were observed. Each succinic acid ligand acts as a μ_4-bridge linking four praseodymium atoms, as shown in figure 1. There are two coordination modes for succinate: (i) each carboxylate adopts a μ_2-η^2-η^1-bridging (one oxygen of the carboxylate connects two metal ions and the other coordinates one metal) coordination mode connecting two praseodymium atoms and (ii) one carboxylate group adopts a μ_2-η^2-η^1-bridging coordination mode, while the other one adopts a μ_2-η^1-η^1-bridging (one oxygen of the carboxylate coordinates to one metal ion, and one carboxylate group coordinates to two metals) coordination mode.

For **1**, there are two crystallographically independent Pr(III) ions in the asymmetric unit coordinating nine oxygens, eight from six carboxylate groups and one from coordinated water molecule (figure 1). Selected bond lengths, angles and torsion angles of **1** are listed in table 2. The Pr1–O distances range from 2.417(4) to 2.577(4) Å with

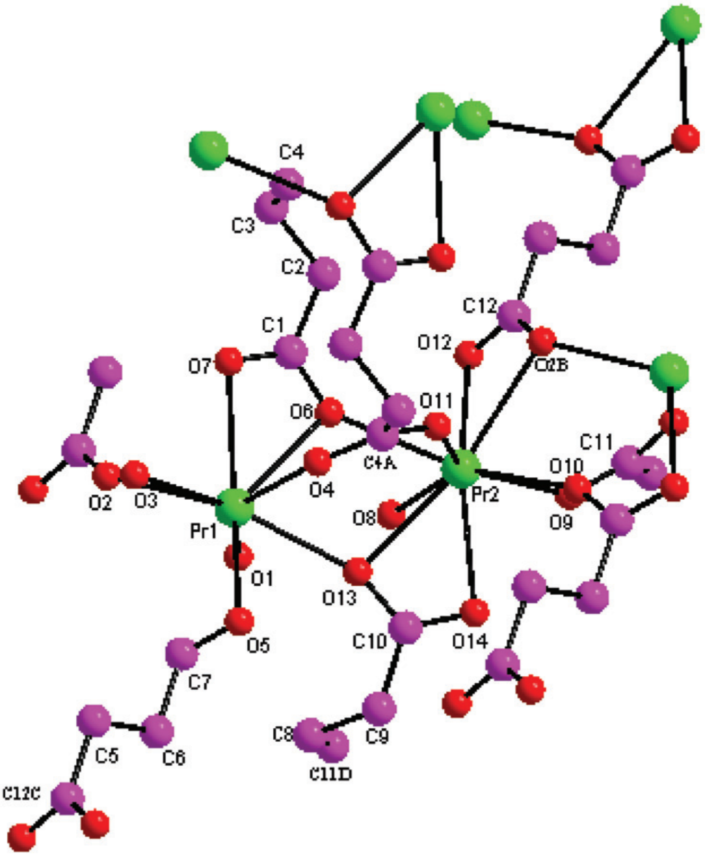

Figure 1. The coordination and linkage modes of Pr(III) ions and succinate in **1**. Symmetry code: A: $1-x$, $2-y$, $1-z$; B: $-1+x$, y, z; C: $1+x$, $-1+y$, z; D: $1-x$, $2-y$, $2-z$.

Table 2. Selected bond distances (Å), angles (°) and torsion angles (°) for **1**.

Pr1–O1	2.531(4)	Pr1–O2	2.512(4)
Pr1–O3	2.542(4)	Pr1–O4	2.417(4)
Pr1–O5	2.521(4)	Pr1–O6	2.577(4)
Pr1–O7	2.530(4)	Pr1–O13	2.450(4)
Pr2–O6	2.474(4)	Pr2–O8	2.500(4)
Pr2–O9	2.428(4)	Pr2–O10	2.479(4)
Pr2–O11	2.471(4)	Pr2–O12	2.538(4)
Pr2–O13	2.626(4)	Pr2–O14	2.529(4)
Pr2–O2B	2.607(5)	C1–O7	1.231(8)
C1–O6	1.304(7)		
C4A–O4	1.249(7)	C4A–O11	1.275(8)
C7–O5	1.229(7)	C10–O14	1.255(7)
C10–O13	1.279(7)	C11–O9	1.237(6)
C12–O2B	1.288(7)	C12–O12	1.231(8)
O4–C4A–O11	125.2(5)	O14–C10–O13	118.5(5)
O12–C12–O2B	121.1(5)	O7–C1–O6	119.6(5)
C1–C2–C3–C4	88.7(5)	C12C–C5–C6–C7	178.9(4)
C11DC8–C9–C10	69.9(6)		

Symmetry code: A: $1-x$, $2-y$, $1-z$; B: $-1+x$, y, z; C: $1+x$, $-1+y$, z; D: $1-x$, $2-y$, $2-z$.

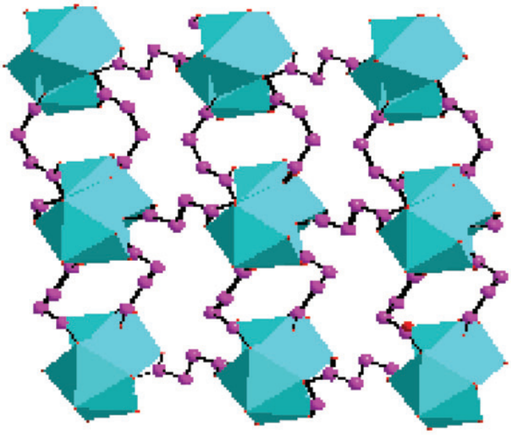

Figure 2. The views of three-dimensional structure of **1**.

average of 2.516(4) Å; the Pr2–O distances are from 2.471(4) to 2.626(4) Å, similar to other Pr–O distances [21]. Carboxylate groups ($-C1O6O7^-$ and $-C12O12O2B^-$) (B: $-1+x$, y, z) have one short distance [C1–O7 = 1.231(8) Å; C12–O12 = 1.231(8) Å] and a long distance [C1–O6 = 1.304(7) Å; C12–O2B = 1.288(7) Å]. The long distances of C1–O6 and C12–O2B are affected by bonding to two praseodymium atoms.

The Pr ··· Pr distance is 4.145 Å in the unit. The O–C–O angles are different [O7–C1–O6 = 119.6 (5)°; O4–C4A–O11 = 125.2 (5)°] (A: $1-x$, $2-y$, $1-z$); the size of O–C–O angles indicates the coordination mode of oxygen atoms. In **1**, there are three independent succinic acid ligands with three conformations established by the related torsion angles, C1–C2–C3–C4, C7–C6–C5–C12C (C: $1+x$, $-1+y$, z) and C10–C9–C8–C11D (D: $1-x$, $2-y$, $2-z$) are 88.7(5), 178.9(4), and 69.9(6), respectively. As shown in figure 2, complex **1** is constructed by succinic acid bridging the chains of edge-sharing P_rO_8 (H_2O) polyhedra to form 3D network structures.

3.4. *Thermal analysis*

As shown in figure 3, thermal decomposition of **1** exhibits three processes. In the range of 130–222°C, 5.50% of weight loss is attributed to the release of two coordinated water molecules (5.42%, theoretical weight loss). The DTA curve of the complex indicates an endothermic process occurring at 186°C. In the range of 393–555°C, an endothermic process at 420 and 469°C corresponds to loss of one succinic acid molecule (observed, 17.46%; calculated, 17.47%). In the range of 737–869°C, the endothermic process at 817°C corresponds to the loss of one CO_2 molecule (observed, 6.61%; calculated, 6.63%). The final residue is the praseodymium oxide and carbon.

The thermal decomposition of **2** also exhibits three processes (figure 4). In the range of 107–415°C, the loss of one free water and two coordinated waters is endothermic, occurring at 179°C (observed, 7.89%; calculated, 7.89%). In the range of 415–571°C, 16.95% weight loss is attributed to the release of one succinic acid (16.96%, theoretical weight loss). The DTA curve indicates an endothermic process at 464°C. In the range of 731–869°C, an endothermic process at 850°C corresponds to loss of one CO_2 moiety (observed, 6.43%; calculated, 6.43%). The final residue is the praseodymium oxide and carbon.

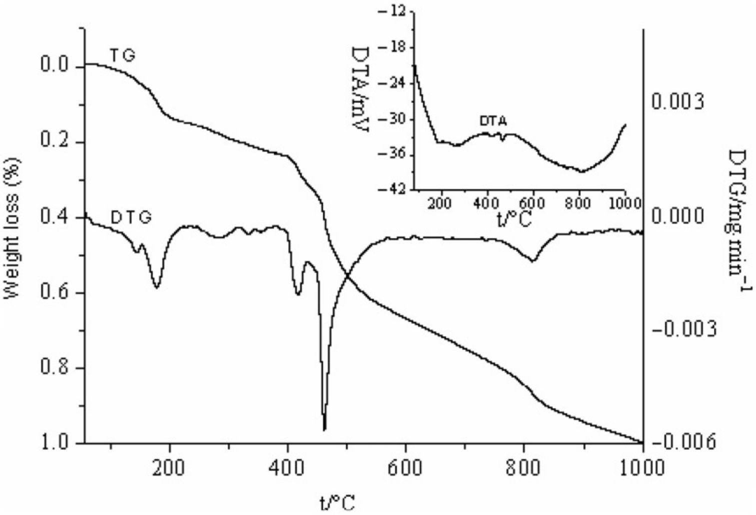

Figure 3. The TG-DTG-DTA curve of **1**.

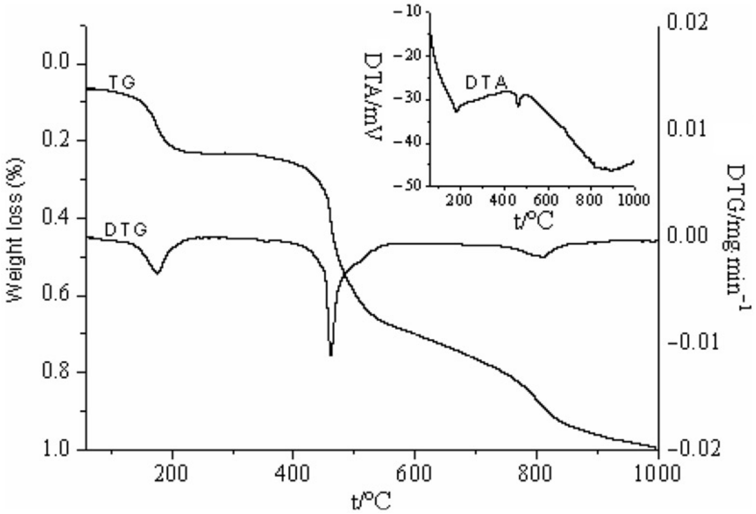

Figure 4. The TG-DTG-DTA curve of **2**.

3.5. *Non-isothermal kinetics*

According to the Achar–Brindley–Sharp–Wendworth and Coats–Redfern methods [25], we analyzed the non-isothermal kinetics. Through comparing kinetic parameters, the possible thermal decomposition reaction mechanisms were examined. The equations of both methods are given as follows:

Equation of Achar method:

$$\ln[(\mathrm{d}\alpha/\mathrm{d}t)/f(\alpha)] = \ln A - E/RT(\mathrm{d}\alpha/\mathrm{d}t = \beta \times \mathrm{d}\alpha/\mathrm{d}T)$$

Table 3. Thermal decomposition kinetic data of **1**.

	The first step			The second step			The third step		
Method	r	E (kJ mol^{-1})	ln A (s^{-1})	r	E (kJ mol^{-1})	ln A (s^{-1})	r	E (kJ mol^{-1})	ln A (s^{-1})
Achar	0.99652	120.378	26.66	0.99195	484.664	75.81	0.99795	1047.073	113.48
Coats	0.98498	143.233	28.06	0.98963	502.980	72.88	0.99593	1076.854	111.51
Average	0.99075	131.806	27.36	0.99079	493.822	74.35	0.99694	1061.964	112.50

Table 4. Thermal decomposition kinetic data of **2**.

	The first step			The second step			The third step		
Method	r	E (kJ mol^{-1})	ln A (s^{-1})	r	E (kJ mol^{-1})	ln A (s^{-1})	r	E (kJ mol^{-1})	ln A (s^{-1})
Achar	0.9833	246.027	62.02	0.98154	221.077	33.97	0.99147	276.714	27.72
Coats	0.9875	273.813	62.21	0.98874	248.231	32.15	0.99781	270.886	21.83
Average	0.9854	259.92	62.12	0.98514	234.654	33.06	0.99464	273.8	24.78

Equation of Coats–Redfern method:

$$\ln[g(\alpha)/T^2] = \ln(AR/E\beta) - E/RT,$$

where α is the degree of conversion, E apparent activation energy, A pre-exponential, β heating rate, T Kelvin temperature, R gas constant, and $f(\alpha)$ and $g(\alpha)$ are kinetic mechanism functions. By calculating the 30 kinetic mechanism functions in equations of the Achar–Brindley–Sharp–Wendworth and Coats–Redfern methods, kinetic parameters E, ln A and r (correlative coefficient) of different mechanism functions were obtained.

Comparing the kinetic parameters of **1** (see table 3), for the first step (number of mechanism functions is 4) E and ln A from Achar method are close to those from the Coats–Redfern method, and both correlative coefficients are good. Corresponding mechanism functions are $f(\alpha) = 3/2 - (1-\alpha)^{2/3}[1-(1-\alpha)^{1/3}]^{-1}$, $g(\alpha) = [1-(1-\alpha)^{1/3}]^2$, respectively, the possible reaction mechanism is three dimensional pervasion $n = 2$, and its kinetic equation may be expressed as $d\alpha/dT = (A/\beta)\exp(-E/RT)\{3/2(1-\alpha)^{2/3}[1-(1-\alpha)^{1/3}]^{-1}\}$. For the second step (number of mechanism functions is 13), E and ln A from Achar method are close to those from the Coats–Redfern method, and both correlative coefficients are good. Corresponding mechanism functions are $f(\alpha) = 1/4(1-\alpha)[-\ln(1-\alpha)]^{-3}$, $g(\alpha) = [-\ln(1-\alpha)]^4$ and the possible reaction mechanism is nucleation and growth $n = 1/4$; its kinetic equation may be expressed as $d\alpha/dT = (A/\beta)\exp(-E/RT)\{1/4(1-\alpha)[-\ln(1-\alpha)]^{-3}\}$. For the third decomposition (number of mechanism functions is 13), E and ln A from Achar method are close to those from the Coats–Redfern method, and both correlative coefficients are good. Corresponding mechanism functions are $f(\alpha) = 1/4(1-\alpha)[-\ln(1-\alpha)]^{-3}$, $g(\alpha) = [-\ln(1-\alpha)]^4$ and the possible reaction mechanism is nucleation and growth $n = 1/4$; its kinetic equation may be expressed as $d\alpha/dT = (A/\beta)\exp(-E/RT)\{1/4(1-\alpha)[-\ln(1-\alpha)]^{-3}\}$.

Comparing the kinetic parameters of **2** (see table 4), for the first step (number of mechanism function is 13), E and ln A from Achar are close to those from the

Coats–Redfern method, and both correlative coefficients are good. Corresponding mechanism functions are $f(\alpha) = 1/4(1-\alpha)[-\ln(1-\alpha)]^{-3}$, $g(\alpha) = [-\ln(1-\alpha)]^4$, respectively, indicating nucleation and growth $n = 1/4$, and its kinetic equation may be expressed as $\mathrm{d}\alpha/\mathrm{d}T = (A/\beta)\exp(-E/RT)\{1/4(1-\alpha)[-\ln(1-\alpha)]^{-3}\}$. For the second step (number of mechanism functions is 29), E and $\ln A$ from A char are close to those from the Coats–Redfern method, and both correlative coefficients are good. Corresponding mechanism functions are $f(\alpha) = (1-\alpha)^2$, $g(\alpha) = (1-\alpha)^{-1}$, respectively, the possible reaction mechanism is chemical reaction, and its kinetic equation may be expressed as $\mathrm{d}\alpha/\mathrm{d}T = (A/\beta)\exp(-E/RT)[(1-\alpha)^2]$. For the third step (number of mechanism function is 9), E and $\ln A$ from Achar are close to those from the Coats–Redfern method, and both correlative coefficients are good. Corresponding mechanism functions are $f(\alpha) = 1-\alpha$, $g(\alpha) = -\ln(1-\alpha)$, respectively, the possible reaction mechanism is nucleation and growth $n = 1$, and its kinetic equation may be expressed as $\mathrm{d}\alpha/\mathrm{d}T = (A/\beta)\exp(-E/RT)\ (1-\alpha)$.

Supplementary material

Tables of atomic coordinates, isotropic thermal parameters, and complete bond distances and angles have been deposited with the Cambridge Crystallographic Data Center. Copies of this information may be obtained free of charge by quoting the publication citation and deposition numbers CCDC: 632762 (**1**) from the Director, CCDC, 12 Union Road, Cambridge, CB2 1EZ, UK (Fax: +44-1223-336033; Email: deposit@ccdc.cam.ac.uk; www: http://www.ccdc.cam.ac.uk).

Acknowledgements

We wish to express our sincere thanks to the National Natural Science Foundation of China (No. 20571036), SRF for ROCS, SEM and Education Foundation of Liaoning Province in China (05L212) for financial assistance.

References

[1] M.H. Cao, C.W. Hu, E.B. Wang. *J. Am. Chem. Soc.*, **11196**, 125 (2003).
[2] M.L. Tong, S. Kitagawa, H.C. Chang, M. Ohba. *Chem. Commun.*, **418**, 4 (2004).
[3] J.S. Seo, D. Whang, H. Lee, S.I. Jun, J. Oh, Y.J. Jeon, K. Kim. *Nature*, **982**, 404 (2000).
[4] T.M. Reineke, M. Eddaoudi, D. Moler, M. O'Keeffe, O.M. Yaghi. *J. Am. Chem. Soc.*, **4843**, 122 (2000).
[5] X. Zhao, B. Xiao, A.J. Fletcher, K.M. Thomas, D. Bradshaw, M.J. Rosseinsky. *Science*, **1012**, 306 (2004).
[6] X.L. Wang, C. Qin, E.B. Wang, Y.G. Li, C.W. Hu, L. Xu. *Chem. Commun.*, **378**, 4 (2004).
[7] L. Carlucci, G. Ciani, D.M. Proserpio, F. Porta. *Angew. Chem., Int. Ed.*, **317**, 42 (2003).
[8] M. Oh, G.B. Carpenter, D.A. Sweigart. *Angew. Chem., Int. Ed.*, **2026**, 42 (2003).
[9] J.C.G. Bunzli, C. Piguet. *Chem. Rev.*, **1897**, 102 (2002).
[10] N. Simon, N. Guillou, T. Loiseau, F. Taulle, G. Férey. *J. Solid State Chem.*, **92**, 147 (1999).
[11] C. Paulet, T. Loiseau, G. Férey. *J. Mater. Chem.*, **1225**, 10 (2000).
[12] N. Simon, T. Loiseau, G. Férey. *Solid State Sci.*, **339**, 1 (1999).

[13] Y. Kim, M. Suh, D.Y. Jung. *Inorg. Chem.*, **245**, 43 (2004).
[14] A. Thirumurugan, S. Natarajan. *Dalton Trans.*, **2923**, 18 (2004).
[15] L.A. Borkowski, C.L. Cahill. *Inorg. Chem. Commun.*, **725**, 7 (2004).
[16] Z.G. Sun, Y.P. Ren, L.S. Long, R.B. Huang, L.S. Zheng. *Inorg. Chem. Commun.*, **629**, 5 (2002).
[17] L. Ma, O.R. Evans, B.M. Foxman, W.B. Lin. *Inorg. Chem.*, **5837**, 38 (1999).
[18] T.M. Reineke, M. Eddaoudi, M. Fehr, D. Kelley, O.M. Yaghi. *J. Am. Chem. Soc.*, **1651**, 121 (1999).
[19] J. Perles, M. Iglesias, C. Ruiz-Valero, N. Snejko. *J. Mater. Chem.*, **2683**, 14 (2004).
[20] J. Perles, M. Iglesias, C. Ruiz-Valero, N. Snejko. *Chem. Commun.*, **346**, 3 (2003).
[21] F. Serpaggi, G. Férey. *Micropor. Mesopor. Mater.*, **311**, 32 (1999).
[22] F. Serpaggi, T. Luxbacher, A.K. Cheetham, G. Férey. *J. Solid State Chem.*, **580**, 145 (1999).
[23] A. Seguatni, M. Fakhfakh, M.J. Vauley, N. Jouini. *J. Solid State Chem.*, **3402**, 177 (2004).
[24] G.H. Cui, J.R. Li, R.H. Zhang, X.H. Bu. *J. Mol. Struct.*, **187**, 740 (2005).
[25] R.Z. Hu, Q.Z. Shi. *Thermal Analysis Kinetics (in Chinese)*, Vol. 47, Science Press, Beijing (2001).